國立臺灣大學理學院大氣科學研究所

碩士論文

Graduate Institute of Atmospheric Sciences
College of Science
National Taiwan University
Master Thesis

土壤溼度與降水耦合現象的先備條件

The preconditions of soil moisture - precipitation coupling in ERA5

陳博元

Bo-Yuan Chen

指導教授：羅敏輝 博士

Advisor: Min-Hui Lo, Ph.D.

中華民國 110 年 7 月

Jul. 2021

國立臺灣大學
大氣科學所
碩士論文
土壤溼度與降水耦合現象的先備條件
陳博元 撰
110
7

國立臺灣大學理學院大氣科學研究所

碩士論文

Graduate Institute of Atmospheric Sciences
College of Science
National Taiwan University

Master Thesis

土壤溼度與降水耦合現象的先備條件

The preconditions of soil moisture - precipitation coupling in ERA5

陳博元

Bo-Yuan Chen

指導教授：羅敏輝 博士

Advisor: Min-Hui Lo, Ph.D.

中華民國 110 年 7 月

Jul. 2021

國立臺灣大學碩士學位論文
口試委員會審定書

本論文係陳博元君（學號 R08229003）在國立臺灣大學大氣科學學系、所完成之碩士學位論文，於民國１１０年７月１２日承下列考試委員審查通過及口試及格，特此證明

口試委員：

（簽名）

（指導教授）

系主任、所長 （簽名）

誌謝

研究很容易會隱約看到一條岔出去卻誘人的小徑就一頭熱地栽進去，以為轉角便是桃花源，回首總卻渾然不覺自己身在何處。研究路上也總是有許多荊棘亂石，對於大學以前早就習慣總有標準答案的我來說，一開始都傷痕累累，心情宕到谷底，而且還延續好幾天甚至幾周。後來我漸漸明白，研究或許是一個人的事，但就像一個王國的建立無法僅靠國王一人，在自己研究的小小世界裡也需要同伴與國師的幫助與扶持才有可能達成。

其中，最要感謝的是指導教授羅敏輝老師。由於我總是以自己的步調前進，不希望因為研究就把生活品質犧牲，一次進度也不會很多。起初很擔心老師會不會覺得這學生很散漫，但時間證明老師給我很多的自由。像是碩士這兩年就去修了三門語言課，或是每天挪用一個小時去寫小說等等。除此之外，當研究卡住時，很常會不敢去找老師，但後來發現每次硬著頭皮去找老師的討論總會有新的眼光與方向，似乎那些擠滿各種思緒的路又被清通，被肯定所做的有價值，被調整腳步能繼續做下去。另外，也特別感謝徐辛學長提供的資料、程式碼和實際的建議，幫助我省下許多 reproduce 的時間，並能站在巨人的肩膀上繼續他的研究。

此外，也非常感謝實驗室的夥伴們，以及從大學一路到碩士的同學朋友們對我研究的建議與日常的關心，特別是我的同窗鈺湄與運動好搭檔秉恩。因為身邊只有你們是最能了解我的研究的人，也因為你們的勤奮讓我沒有懈怠的理由。

在五月疫情爆發之後，也是最後研究的衝刺期，感謝室友雋閎與昶劭無私而精湛的廚藝，讓我不用擔心每餐要吃什麼，只需要幫忙就好。

除了直接對這篇研究幫助的感謝之外，我也要感謝教會持續為我禱告的朋友。每次我提的代禱事項必定有研究，但你們總不厭其煩地持續為這事守望，也常常時不時以行動支持，讓我感到很窩心、也在那些精心的時刻中被充電，即便在疫情爆發後仍持續透過線上的方式彼此紀念。

而家人雖然遠在南方，但非常感謝父母在經濟上全力支持，叫我不要擔心錢的事，使我能專心來研究。而許多愛的舉動也讓我非常感動，諸如每次為省錢搭末班高鐵回家但父母仍堅持專車接送、張羅三餐和水果、又在他們睡午覺的時間專車在

我回去。

最後，我要感謝上帝。當我發現研討會報告被排在去棲蘭半個禮拜後的當天下午時，我請朋友一起禱告，事就順著成了；當我發現自己情緒很容易受研究結果的好壞影響時，我和朋友一起禱告，負面情緒從延續一周，一路縮短只剩不到一小時就能完全調整好；而在疫情氾濫，身體健康與人心中的計畫都顯得稍縱即逝之時，更顯得這篇研究的完成並非僅憑人的努力就能順利完成。

抱歉或許遺漏某些應當感謝的人，在這裡我也一併感謝。這兩年世事變化難料，感謝所有曾經直接或間接幫助我的，才能讓這篇研究在大海翻騰時仍順利誕生。

中文摘要

由於地表條件作為提供大氣能量的主要來源，且與人類生活密切相關，自 1990 年代以降便受到越來越多關注。藉由衛星與模式資料，許多過去的研究指出下午降水傾向發生在早晨土壤比較濕的時候，但在土壤比較乾的地方。這很可能肇因於在乾土壤上空，地表溫度在空間上的異質性所激發的輻合、隨後發生的上升氣流、以及在這段較氣候值為潮濕的時期，較多水氣可供蒸發。近期研究進一步發現，當某些土壤條件滿足時，所謂的「空間上土壤溼度與降水之負回饋機制」會變成正回饋。然而，由於某些重要變數很難獲得全球尺度的觀測資料，諸如地表通量、溫濕度在高度上垂直的變化等，這兩種正負回饋機制在現實中是否僅在降水發生當天就被建立起，至今很少被討論。為了連結觀測與模式、並釐清前幾天大氣與土壤濕度的狀態， ERA5(ECMWF Reanalysis 5th Generation)再分析資料將被使用在本研究的大部分內容中。統計結果顯示無論是哪一種回饋機制，都在背景環境的發展中存在溫度及絕對溼度的正距平，這不是直接來自當地就是來自白天透過對流的傳送。兩正負回饋機制的差異在於：正回饋因為有較豐富的水氣，大氣會先被加濕並藉此累積能量；而負回饋的加濕與積能速度更快，卻僅發生在能透過強烈對流從周遭將水氣帶入的降水事件當天。這導致在事件當天早上的大氣加濕現象，正回饋從地表往上到大氣中；而負回饋則先從大氣開始加濕，再延伸至地表。雖然只使用一種再分析資料，且仍舊無法下因果的結論，本研究突顯在前幾天先備條件的重要性，並顯示很可能與在事件發生當天空間上的回饋機制有關。

關鍵詞：陸地大氣交互作用、ERA5、土壤溼度、午後降水、回饋機制

ABSTRACT

As playing a critical feedback role to the atmosphere and closely relating to human life, land surface condition draws more and more attention since the 1990s. Based on satellite data and idealized model results, many previous studies stated that precipitation in the afternoon tends to occur when soil is wetter and where it is dryer. This is probably because of the convergence induced by spatial surface temperature heterogeneity and the subsequent updraft over dryer soil, as well as more available water vapor evaporated during wetter period. A recent study further shows that this negative "spatial soil moisture – precipitation feedback (spatial SM-P feedback)" may shift to positive when some soil conditions fulfill. Nevertheless, whether the development of both positive and negative spatial SM-P feedback emerges merely on the morning of the afternoon precipitation event or not is rarely discussed so far. It is because the lack of variables in observation that hard to be obtained globally, and because of the necessity of sufficient computational resources if using model. To act as a bridge between observation and model results, and figure out what had happened before the event day, ERA5, a state-of-the-art reanalysis data released only in recent years, is used in this study. Statistical results show that no matter the coupling is positive or negative, there is development of positive temperature and specific humidity anomaly, which can help destabilize the low atmosphere in the first place. The difference is that positive coupling moistens the air and accumulates energy which starts earlier due to the presence of richer soil moisture while the negative does it faster only on the event day with the help of fiercer convection that brings moisture in from the surroundings. This causes the moistening on the event day morning from the wet surface up to the atmosphere under positive cases while causing the moistening first

happened in the atmosphere then down to the dry surface under negative ones. Though applying only one reanalysis data and not including firm causality, this study highlights the importance of the preconditions in the previous days. This may help improve the knowledge of spatial SM-P feedback, which may apply to forecasts on short to medium range, and climate change.

Key words: Land-Atmosphere Interaction, ERA5, Soil Moisture, Afternoon Precipitation, SM-P feedback

CONTENTS

LIST OF FIGURES

Chapter 1 Introduction

Energy reached the Earth is offered primarily by Sun (Fitzharris, 2001). However, almost half of it penetrates the atmosphere, absorbed by Earth's surface, and later released back into the atmosphere in the form of radiation, sensible heat, and latent heat (Kiehl and Trenberth, 1997). The partition of the latter two components affects local as well as global weather and even climate tremendously. The dry and wet two heat fluxes contribute to may also shape human's life. So it is essential to understand in advance how atmosphere reacts to the change of the partition, and the impact of every decision we make related to this change. Owing to the potential importance, what role the land plays in the land-atmosphere interaction gradually attracts more and more focuses in the last three decades (Nicholson, 2015) so as to make more precise decision and prediction.

A great attention has been paid to the interaction between the state of soil moisture and of the subsequent rainfall due to its importance for driving land-atmosphere feedback and playing a key role in climate system (Nicholson, 2015; Seneviratne et al., 2010).

Back in 1980s and 1990s, based on observation, it was believed that rain tends to occur at the antecedent wetter soil, which was later called as positive soil-moisture precipitation feedback (positive SM-P feedback) (Eltahir & Bras, 1996). The reason why it happens was regarded as moisture recycling; that is, precipitation water falls back to where it evaporated (eg. Findell and Eltahir, 1997; Eltahir & Bras, 1996; Taylor & Lebel, 1998) with the help of more water vapor and existing convergence gathered in the lower atmosphere (Taylor et al., 1997).

Nevertheless, as satellite data became available, detailed and global information was revealed. Taylor et al. (2011) found that the initiation of Mesoscale Convective Systems (MCS) in the Sahel in daily time scale prefers locating at the upwind side of dry-to-wet

soil moisture anomaly and high-to-low surface temperature anomaly transition. This negative SM-P feedback was further confirmed via global satellite data in Taylor et al. (2012). Fortunately, the seeming contradiction was successfully reconciled by Guillod et al. (2015). By means of global satellite data, Guillod et al. (2015) discovered that, in general, afternoon rain prefers occurring when it is wetter (positive temporal SM-P feedback) and where soil is dryer compared to the sounding regions (negative spatial SM-P feedback) in the morning. Following those works, Hsu et al. (2017) further stated that though generally negative, spatial SM-P feedback tends to become positive as morning soil moisture becomes wetter in temporal and as the heterogeneity becomes lower in spatial. These four important papers give a broad view on the tendency of soil moisture distribution when precipitation happens. Still, they all have difficulties unveiling the exact links hidden in the atmosphere between morning soil moisture and afternoon rainfall. This may be due to the lack of some key observational information globally such as surface fluxes, vertical profile. There are also some long-recognized issues such as difficulty to isolate processes, to gain a solid causality out of rather complicate earth system (Seneviratne et al., 2010; Nicholson, 2015; Wei & Yang, 2016), and to include wind effects on the SM-P feedback (Froidevaux et al., 2013; Holgate et al., 2019; Lee et al., 2019).

Numerous idealized model studies have been trying to track down the mechanism behind since the 2000s. The surface heterogeneity-induced wind (such as vegetation (Garcia-Carreras et al. 2010), soil moisture (Taylor et al. 2007), and temperature found in observations) may trigger the convection (Garcia-Carreras et al. 2011), and potentially lead to subsequent rainfall (Froidevaux et al., 2013; Lee et al., 2019). This also made way for the explanation of why precipitation occurs over dryer soil (Taylor et al., 2011). First, horizontal temperature gradient toward dryer soil induced near-surface wind flow from

wetter soil to drier one, carrying vapor to moisten the atmosphere over dry soils. With more buoyancy released directly from dry soil and moisture converged from the neighboring, the tendency of convection develops. Last but not least, the convective clouds then pop up, mature and bring precipitation on the same dry soil, completing a negative spatial SM-P feedback. However, most of them only set different atmospheric or land scenario or use data relevant to a particular event to see the individual impact. How the advantage of precipitation forms especially in previous days globally is seldom mentioned so far. In addition, whether the mechanisms based on the idealized model can be totally applied to reality is still unknown.

In light of this, the goal of this study is to better know the ins and outs of the spatial SM-P feedback in both temporal and spatial perspectives using the atmospheric reanalysis datasets. In section 2, data and methods applied are introduced to identify afternoon rain events, along with the introduction of the definition of spatial SM-P coupling in temporal and spatial aspects. Results in section 3 analyze the environments of both positive and negative SM-P feedbacks by means of these two perspectives respectively after the data validation. Integrating both aspects, the discussion in section 4 only split into positive and negative cases to reveal and compare the evolution of each. Section 5 summarizes the important findings of this study.

Chapter 2 Methodology

10 years global data ranging from 60S to 60N and in the period of 2002-2011, including satellite and reanalysis, are adopted to comparison and analysis. Recently-released reanalysis data from European Centre for Medium-Range Weather Forecasts (ERA5), which are constrained by observational data of many sorts, are mainly used in this study. It has very high temporal (hourly), spatial (0.25°×0.25° in horizontal direction, 137 levels in vertical direction) resolution globally. To compare the similarity of the soil moisture condition between observation and reanalysis, microwave satellite observational precipitation data are used from the Climate Prediction Center morphing method (CMORPH) (Joyce et al., 2004), whose temporal and spatial resolution are 3-hourly and 0.25°×0.25°, respectively; and evaporative stress from Global Land Evaporation Amsterdam Model (GLEAM) (Miralles et al., 2011), later adjusted by Guillod in 2015, is applied as an index of surface soil moisture, with the same spatial but daily temporal resolution. The first two data are rearranged into local time beforehand to ease the procedure of identifying afternoon rain events. As for the soil moisture, 9am local time data were used in both ERA5 and GLEAM dataset.

Because the goal is to find the surface condition in the morning when afternoon precipitation takes place, rain events were selected and filtered before analysis. An event candidate was detected if the accumulated afternoon rainfall (12-23LST) exceeds 4mm, and one in the morning (6-11LST) is below 1mm, in order to identify significant rainfall and to remove any contamination of soil from morning rainfall, respectively. The duration and the threshold chosen follows Hsu et al. (2017), which should be flexible. Next, 5x5 box method, that is, a square region with 5 grid points on both sides centered at maximum afternoon rainfall, was set to later examine the spatial conditions of land and atmospheric

variables. The selection of 5 grid points is made because soil moisture distribution at scale of around 150km is also proved to have obvious impact on later convective precipitation(Taylor and Ellis, 2006). Then, to get pure influence of daily SM-P coupling as possible, a candidate was removed if water body exceeding 5%, or the maximum altitude difference exceeding 300m within that 5x5 candidate box. Global land cover and topographic information are taken from ETOPO1 (Amante and Eakins, 2009) and GLC2000 (Bartholomé and Belward, 2005) with the spatial resolution of 1 arc-minute (~0.017°) and 1km (~0.009°), respectively. In addition, candidates that occurred above 950hPa, or 600m, were also removed to reduce any possible influence which may arise from the altitude. The distribution of the regions topographic constraints listed above are illustrated in figure 1. Valid regions shaded by both light and dark green include long-recognized hot spots such as Sahel in West Africa, Great Plain in central US, northwestern part of India (Koster et al., 2004), as well as other semi-arid regions like Pampas, Western Australia and Eurasian steppe. But there are other climate zones included such as a large part of western Amazon and European Plain. In the end, there are around 48,000 cases remained and used to analyze later, which is served as sample size.

After soil moisture values were first sorted by percentile, which SM in each case is sorted from the lowest to the highest for the purpose of being dimensionless, ranging from 0 to 1, Inward Soil moisture Gradient (ISG), introduced by Hsu in 2017, was used to estimate the spatial distribution of morning soil moisture condition at 9am as following:

$$\mathrm{ISG} = \sum_{i,j} \frac{S_{L_{00}} - S_{L_{ij}}}{\sqrt{i^2 + j^2}}, for\ i,j = -2,-1,0\ 1,2$$

where S is soil moisture percentile. Subscript L_{00} is at the center of the 5x5 box(or "the core") where the maximum afternoon rainfall occurs while i and j denote the relative

distance between L_{00} and the rest of the 24 grid points. According to the equation, ISG increases as SM at the core increases. Therefore, combining these two methods, spatial SM-P coupling index can be finally defined as ISG. That is, positive ISG indicates positive spatial SM-P coupling for the maximum afternoon rainfall is located over wetter soil at the core of the 5x5 box; and vice versa.

Other variables will later insert into the equation to give a view of the spatial environment before and after the rain events at section 3.2 and 3.3, and the 0.05 two-tailed significant T-test is applied in the evolution diagrams. Temporal environment will also be shown to better know the deviation relative to its climatology after removing its seasonality.

There are other things needed to note in advance. First, to achieve consistency, the analyses in section 3.2 and 3.3 were conducted only by ERA5 data. Second, “SM-P coupling” will be used instead of “SM-P feedback” owing to the unknown of causality when using statistic methods. Lastly, the “atmosphere” mentioned below is only for low atmosphere at the same resolution of 25hPa from 975hPa to 800hPa.

Chapter 3 Results

A comparison of the relationship between morning SM condition and afternoon precipitation between observation and reanalysis data will be taken in the first part. Then the analyses of environmental conditions under different morning ISG (at 9LST) and their evaluation will be divided into two subsections: temporal and spatial perspectives. Within each of them, the impact of ISG at a fixed time (11am in this study) and of time in both composite positive and negative ISG on variables, e.g., surface heat fluxes, near surface conditions, all the way up to thermal, dynamic, and energy states in the low atmosphere are examined in turn.

3.1 Comparison between observation and reanalysis data

In order to figure out the performance of ERA5 on the spatial SM-P feedback, the result in Hsu et al. (2017) is made use of and modified (the units of soil moisture in GLEAM and ERA5-L are both replaced by percentile). Figure 2 displays what the morning soil moisture anomalous condition is when the afternoon rain events occur. For the observation illustrated in Figure 2a(i), the percentage of positive spatial SM-P coupling rises as the maximum soil moisture anomaly increases along x-axis while it declines as the SM heterogeneity decreases along y-axis, which is similar to that in Hsu et al. (2017). This tendency can also be captured in ERA5 demonstrated in Figure 2b(i) qualitatively, but not quantitatively. This indicates that comparing to observations, there are more rain events occurred over spatially wetter soil in ERA5. However, ERA5 does show the existence of the tendency of spatial SM-P coupling in temporal and spatial aspects. It just fails to capture to what extent the dominant mechanism should shift from the positive coupling to the negative one, or in the other way. Therefore, the mechanism

behind the results is supposed to be correct and practicable to continue the following investigation.

In addition, the distribution of the observational case number in Figure 2a(ii) is similar to that in Hsu's paper. Though the distribution from ERA5 in Figure 2b(ii) contains less cases of high SM heterogeneity than that from observation, both distributions are alike where SM heterogeneity is lower than 0.1. That is, the analyses conducted below is still appropriate to interpret rain events whose SM heterogeneity is smaller than 0.1.

3.2 Temporal analysis

Event condition comparing to its climatology is worth spending efforts on in the first place to know how anomalous it is under different ISG right before the rain event takes place, that is, at 11LST.

Variables at and near the surface are examined first due to the expectation of keeping most of the signals from the surface characteristics, or ISG particular in this study. Indeed, soil drier (wetter) than the surroundings, that is, ISG < 0(ISG > 0), does correspond to higher sensible heat flux that transports into the atmosphere(soil) and higher latent heat flux that transports into the soil(atmosphere) in Figure 3a. Two lines cross when ISG is negative but close to 0. On the contrary, the total heat flux does not change much and fluctuates around 0. Although the spread of 95% cases is large, the trends are rather clear.

The deviation of latent and sensible heat fluxes goes upward and may contribute to near surface specific humidity and temperature, respectively (Fig. 3b). Interestingly, though positive ISG cases correspond to lower temperature relative to negative ones, the average of the temperature at 2m height is mostly positive. Specific humidity is also generally positive and maximized at extreme ISG. But it can still be seen that lower

(higher) value tends to located at negative (positive) ISG. The spread is also large, but the spread of specific humidity is much smaller than that of temperature, and shows much clearer ascending trend as ISG grows. Note that two lines in Fig. 3b use different scale of y-axis.

Things change when climbing up to the lower atmosphere. The tilt existing in Fig. 3b disappears in Fig. 4a. Though there is still a slight tendency for temperature to decline toward positive ISG and toward higher level, specific humidity in the atmosphere is almost homogeneous across different ISG and pressure levels. The ambiguity does not happen when it comes to the dynamic part in Fig. 4b. Below 900hPa, convergence can be seen almost everywhere. Stronger convergence associated with also stronger upward motion exists in negative ISG while the convergence and updraft are weaker in the positive side. Above 900hPa, divergence and downdraft occur at certain extreme ISG intervals with even stronger divergence situated at the side of negative ISG. But in general, there is no apparent tendency within this layer.

We next explore whether these features at 11LST are formed merely on the morning of that particular event day or not.

The evolution of land and atmosphere under positive and negative spatial SM-P coupling diverges from each other. For the positive coupling in Fig. 5(a), 3 days before the event happens, temperature starts rising in the low atmosphere, corresponding to the positive deviation of soil water close to the surface layer and slowly accumulated water vapor in the low atmosphere. One day later, temperature rises even higher not only in atmosphere but also underground. Noted that the diurnal cycle has removed as values shown here are all anomalies, which indicate that the daytime heating in these days is far more intense than it used to be. However, a rather rapid moistening happens in the atmosphere, which may lead to rain in the evening as there is an increase of soil moisture

near the surface in the afternoon. But it does not hinder the precipitation due to the positive deviation of all four variables no matter in soil or atmosphere on the event day morning. The signal of dropping temperature extends from the surface up into the atmosphere and down into deeper soil, which lasts at least until the following day.

Unlike the positive coupling abundant in moisture, there is much less moisture under negative coupling as shown in Fig. 5b. Nevertheless, the atmospheric moisture shows a positive deviation at first. In addition, the negative coupling has a corresponding much higher soil temperature anomaly, which later propagates upward into the atmosphere mainly in daytime, causing an increase of air temperature away from its climatology. Though the accumulation of moisture in the atmosphere lags that of temperature for one day, it finally starts two days before and maximizes on the morning of the event day. In the meantime, soil temperature near the surface continues rising while soil moisture dropping. On the beginning of the event day, though the moisture in soil and the atmosphere are both much lower than that under positive coupling, the overheated surface rapidly heats the atmosphere, inducing strong convection, bringing lots of moisture from the surroundings. In the end, it still creates a good environment for precipitation to take place. The cooling also happens after rain events in the following day just as what has happened under the positive coupling.

Investigating the dynamic part in Fig. 6 may further assist in the construction of the whole picture. Although convergence and updraft both exist especially in daytime and maximize on the event day under positive and negative coupling, those under negative coupling are stronger and more regularly-appeared than under positive one. Another interesting feature is the location of maximum convergence in the previous days. It locates at around 900hPa under positive coupling while situates near the surface under negative one. Divergence and downdraft anomaly can mainly be found on the afternoon of the

event day and the following day under both couplings, indicating the presence of precipitation.

Fig. 7 shows the evolution of Moist Static Energy (MSE) in the atmosphere, which can demonstrate the changes in energy in previous days. MSE under positive coupling grows first. One day before the event, it even reaches more than half of its maximum value appeared on the event day. The advantage under positive coupling emerges earlier than that under negative one. However, it is “overtaken” by negative coupling on the event day. Most of the MSE accumulated under negative coupling is gained on the event day and maximizes at the upper part of the low atmosphere. In addition, based on Fig. 7a, c and 7b, d, the changes in MSE are both mainly contributed from specific humidity, which is higher under positive coupling a day before but even higher under negative coupling on the event day.

The different MSE trends can further be verified in Figure 8. In diagram (a), the average of convective available potential energy(CAPE) anomaly under negative coupling cases is lower than that under positive from the beginning. The difference maximizes during the afternoon before the event day(-12hr to +0hr) which the positive reaches its peak. But on the event day, the CAPE anomaly of two types of coupling both rises up to around 350(J/kg) and drops almost in the same way. In diagram (b), he convective inhibition(CIN) in two scenario fluctuates in first two days. Then the CIN of negative coupling rises higher than that of positive one, right before a great drop on the event noon.

Now we know the spatial SM-P coupling is likely to happen generally when there are positive deviations of temperature, moisture, convergence and updraft in the atmosphere no matter under positive or negative coupling. Then the next question is: In what kind of position is the event likely to happen?

3.3 Spatial analysis

Spatial distribution of those variables mentioned above is of equal importance due to its impact on the key roles of surface-induced wind and the subsequent updraft that may determine many precipitation characteristics, such as location, strength, and spatial scale in some cases (Garcia-Carreras et al., 2011, Lee et al., 2019). In this subsection, positive (negative) value represents the variable at the center point of the 5x5 box (L_{00}, or "the core") is larger (smaller) than its surroundings at 11LST on the event day. "Higher" and "lower" refer to that at the core comparing to its surroundings in this subsection.

Although the trends in Fig. 8 is similar to that in Fig. 4, they have a different meaning. For negative coupling, sensible (latent) heat flux is higher (lower) in Fig 8a, but it drops (rises), and shifts to the opposite situation as ISG becomes positive. The results are obscure when ISG is almost 0. It agrees to the definition of ISG that under positive (negative) ISG, wetter(dryer) soil at the core is supposed to have more latent (sensible) heat flux than the surroundings. Total surface flux experiences little increase as ISG grows, meaning that it transports less (more) surface flux at the core when ISG is negative(positive). Similarly, at near surface, higher (lower) temperature and lower (higher) specific humidity co-exist in negative (positive) coupling in Fig. 8b, which is consistent to our knowledge. As for the spreads of both diagrams in Fig. 8, they are still very large yet with a clear tendency consistent with their average.

The contrast between positive and negative coupling reveals in the low atmosphere (Fig. 9a). Under negative coupling, higher temperature but lower water vapor are below 900hPa, corresponding to generally stronger convergence and updraft in Fig 9b. Above 900hPa, there are lower temperature, higher moisture and downdraft gathered. On the

contrary, positive coupling contains lower temperature and higher humidity which are both maximized at around 950hPa, but the signals dissipate away from this level. The strength of convergence and vertical velocity is spatially homogeneous below 900hPa, but is staggered above.

In fact, the dipole of thermal terms between positive and negative coupling below 900hPa at 11LST on the event day may gradually be established a couple of days before (Fig. 10a). In positive coupling, soil moisture is always higher and soil temperature is always lower, but moisture and temperature in the atmosphere are both close to zero in the beginning. Soil temperature becomes lower while the near surface atmospheric humidity reaches local maximum every afternoon, which is eliminated regularly at night. However, in spite of the elimination, the signals gradually propagate downward and upward respectively, and even start accumulating. Lower temperature gradient starts to show up one day before the event. On the morning of the event day, though temperature is still lower both in soil and the air, moisture already abundant in the atmosphere rapidly rises from bottom to top and rainfall occurs in the end. What happens in negative coupling is a bit complicated yet similar to that in positive coupling only in an opposite way in Fig. 10b. Soil moisture is instead always lower before the event, corresponding to higher soil temperature near the surface, which dries and heats the atmosphere regularly every afternoon. The signals are eliminated overnight, which is similar to what has happened under positive coupling. However, the amplitude of the drying and heating signals every afternoon is enhancing until the event occurs. Another trait worth noting, which shows a similar pattern is the lower temperature but higher moisture in the upper part of the low atmosphere. Higher air temperature finally shows up near the surface one day before the event. On the event day morning, rapidly-increased air temperature corresponds to moistening from top to bottom in the atmosphere, and then precipitation still occurs. The

different development of strategy to produce rainfall may lead to the dipole shown in Fig. 9a.

Both diagrams illustrating the dynamic perspective of positive and negative coupling in Fig. 11 show similar results though some differences remain. Convergence is generally everywhere but not for vertical velocity. Before every noon, downdraft and updraft occupy below and above 900hPa, respectively. In the rest of the day, situation reverses. This phenomenon is more obvious under negative coupling. As time goes by, the updraft below 900hPa in the afternoon grows stronger and earlier, especially under negative coupling. As for the difference in convergence, stronger convergence starts to appear and develop above 900hPa every afternoon only under positive coupling while significant convergence only happens on the event day afternoon under negative coupling.

From energy perspective, different kinds of development can be clearly seen in Fig. 12. For the positive coupling, higher MSE appears every afternoon and becomes even higher in the following days, which mainly comes from specific humidity while the contribution of temperature is negative but smaller (Fig. 12a, b, c). The elimination of specific humidity gradient can be seen during the night but again is interrupted by MSE rising in daytime. On the event day, MSE rapidly rises from bottom to top and is maximized at near surface as moisture does and releases when precipitating. On the contrary, MSE under negative coupling is mostly lower at the core before the event, which is also mainly contributed by specific humidity. Interestingly, temperature term does not show positive contribution to the MSE until the afternoon of the previous day, which is so minor to offset the overwhelming influence of the lack of moisture (Fig. 12e, f, g). On the event day morning, however, MSE still rises but from top to bottom as specific humidity does and maximizes at upper part of low atmosphere.

The energy trend can also be seen by CAPE and CIN in Fig. 13. Under positive

coupling, CAPE is higher at the core and even higher every afternoon. On the contrary, the surroundings contain more CAPE under negative coupling, which become highest every afternoon. Yet on the event day afternoon, the CAPE gradient under negative coupling switches to positive even though the value can not as high as that under positive one. On the other hand, CIN gradient under negative coupling is often higher than that under positive until the event day afternoon.

According to the last subsection, we know that rain events happen when there is enough thermal energy in the atmosphere including temperature and moisture anomaly which have developed days before, and when dynamic terms including convergence and upward motion exist. Here we further find two more crucial facts. First, the higher (lower) soil moisture gradient under positive (negative) coupling may first transport more latent (sensible) heat into the atmosphere and cool (heat) surface soil concurrently as well as the air near the surface one day before the event in daytime. Next, under negative coupling, stronger concentrated updraft at the core may lead to the moistening at the upper part of low atmosphere, which happens earlier than the moistening at the lower part.

Chapter 4 Discussion

The rain events discussed here are those there are no precipitation in the morning (6-11am) but significant in the afternoon (12-23pm), which take places on low (altitude<600m) and flat (altitude difference<300m) land between 60N and 60S globally based on the events from 2002 to 2011. Though complicated and inherent in Hsu et al. (2017), the filter still has its own limitations. One is it can only mitigate the influence other than land-atmosphere coupling such as land-sea contrast, topography, and large-scale weather system. The other is that it is unknown which type of cloud causes the precipitation, whether it is stratified or merely convective cloud. In addition, turbulence is not considered in this study due to the boarder resolution of 30km, which may be important sometimes (Garcia-Carreras et al. 2011).

To reach consistency, most of the results are purely based on ERA5 reanalysis data. Though assimilating lots of observations, it can not be equal to the reality due to the long-recognized issues of resolution, parameterization (Taylor et al., 2012), and energy balance closure problems (Foken, 2008). For example, the location and the amount of precipitation are not totally the same as what had really happened over the land. However, due to the result that the dominant mechanisms behind the spatial SM-P coupling should be similar, which is discussed in section 2, the tendencies of two kinds of coupling may still be found in observation if there is, and the results can still be applied at least qualitatively.

4.1 Positive spatial SM-P coupling

The background of spatial positive coupling is the higher soil moisture anomaly concentrated at the core which extends down to the bottom of the available layer, and the higher mean state of moisture anomaly in the air comparing to the negative coupling,

which is as expected. However, an unexpected rising temperature anomaly in the atmosphere emerges three days before the event. It heats the air homogeneously and is probably not mainly from local due to the lack of temperature gradient within the 5x5 box. No matter where it comes from, it shapes the distribution of MSE anomaly on the first two days and may give the opportunity for later development.

Meanwhile, there are two phenomena that may indicate the presence of rather strong latent heat flux: the cooling at the surface soil and the moistening in the atmosphere near the surface every afternoon. This may contribute to the accumulation of near surface specific humidity and MSE anomaly in daytime, destabilizing the atmosphere. Though the cooling at the surface soil exists, heating from sun still rises the soil temperature anomaly. Though the moistening in the atmosphere near the surface is regularly interrupted at night, this moisture gathering still effectively increases moisture across the 5x5 box homogeneously compared to its climatology.

One day before the event, the air temperature anomaly accumulated by the mechanism mentioned above reaches its first peak at around noon, followed by the atmospheric specific humidity anomaly as stronger convergence and updraft debut later in the afternoon. With the advantage of sufficient thermal and dynamic input, MSE anomaly rises gigantically and further destabilizing the atmosphere during the day despite the cooling which probably results from evapotranspiration and pioneering rainfall. Perhaps the rain help further moistens the near surface air instead owing to the minor loss of specific humidity and MSE anomaly.

Temperature anomaly reaches its second peak again probably by means of the same mechanism on the event day morning but with a much better atmospheric condition to develop. High CAPE and low CIN not only in temporal but also in spatial perspective perhaps help trigger even stronger convergence and updraft. It may pump the moisture

inherited from the pioneering rain from near surface to deeper low atmosphere and eventually moisten every level. As the precipitation takes place, moisture and the corresponding MSE both hit their peaks in the afternoon.

In the end, precipitation releases energy and moisture in the atmosphere but greatly moistens shallow soil and cools temperature in the soil and the atmosphere alike, yet not for the soil moisture gradient, or heterogeneity. It may indicate that the type of rainfall may be relatively-homogeneous, or wide-range.

4.2 Negative spatial SM-P coupling

If the positive coupling is aided by the increase of temperature from outsiders to prepare an event, a negative one then may be almost on its own, except the positive specific humidity anomaly already existing in the atmosphere.

The most different feature under negative coupling in the first two days is the lower state of soil moisture anomaly and gradient, which can be seen all the way down to the deepest soil layer available. With no water to evaporate, surface is rapidly heated especially at the core in the afternoon and releases lots of sensible heat into the air, which is rather homogeneous across the 5x5 box. The strong heating near the surface may also cause the low CAPE and high CIN at the core relative to the positive cases. However, the heating from the surface deviates air temperature away from its climatology from bottom to top, being the major contributor of MSE in the first part. Though the hot temperature may induce convergence and updraft and gather the moisture very close to the surface from the surroundings, the signal soon dissipates probably in order to offset the lack of moisture in the soil as possible. Again, the coming night breaks the development regularly. There might be radiative cooling to mitigate the overheating both in soil and the atmosphere. The negative gradient of moisture in the air is also redistributed. But the

positive deviation of temperature anomaly stands and continues dominating the shape of MSE.

Despite the incident during night, instability (CAPE anomaly) and the strength of convergence and updraft continues intensifying by the higher temperature anomaly. One day before the event, moisture eventually starts accumulating in the atmosphere, dominating the development of MSE. In the same time, air temperature anomaly rises even faster in daytime especially near the surface and hits its first peak. Slight yet still existing pioneering rainfall may also inject some moisture near the surface to further destabilize the atmosphere.

In fact, MSE, CAPE at the core has not been the highest relative to its surroundings until the event day morning. It may be the strong circulation ascending fiercely at the core that gathers moisture and energy effectively from the surroundings. The intense moistening happens first in the upper part of the low atmosphere, obtaining most of the MSE merely in this short period comparing to its maximum. The cycle of accumulating energy lasting for days finally ceases as soon as the afternoon rain events occur.

There is one thing in the aftermaths worth mentioning. The precipitation drenches the ground only at the core due to the fact that the originally extreme negative gradient of soil moisture shifts to even extreme positive, enlarging the soil moisture heterogeneity, which is absent under positive coupling. This finding is consistent with Hsu et al. (2017). It may also indicate the scale of precipitation is different under positive and negative coupling.

4.3 Comparing the preconditions

Here we would like to highlight major similar and different points between the opposite couplings, as a schematic diagram in Figure 13.

At background and developing state, positive coupling wins in thermal term while negative one in dynamic term. Positive coupling gets a head start on specific humidity anomaly released mainly from soil close to the core. With enough warming, convergence, updraft, and the extra moisture coming from the pioneering small-scale rainfall, water vapor is effectively gathered from surface and leads MSE, destabilizing the atmosphere by the increase of CAPE anomaly and decrease of CIN gradient. At the mature state, CIN anomaly still grows at first. But with the lower energy barrier relative to its surrounding (negative CIN gradient), when convergence and updraft that are strong enough emerge, MSE, mostly collected on the previous day, is finally released in the already-destabilized environment and leads to significant precipitation at that specific position.

Under negative coupling, though first at disadvantage, drier condition in the soil induces higher temperature and stronger convection comparing to positive coupling, still drawing water vapor from the surroundings at developing state. Though generally CAPE is lower and CIN is higher no matter in anomaly or gradient, convection stronger than that under positive cases on the event day morning still breakthrough the barrier, which this result is consistent with what Garcia-Carreras found when comparing mechanisms in different scenario of atmosphere stability in 2011. Coupled with the benefit of already positive specific humidity, moisture and MSE are gathered rapidly from the surroundings on the event day morning, which triggers precipitation in the end.

Despite the differences primarily arisen from under the surface, similarity remains and is vital between them, especially occurred in the atmosphere. They both have positive temperature and moisture anomalies throughout all three state before the event. No matter where the signals come from, they are both intensified generally due to the presence of convergence and updraft in daytime, dissipated overnight, yet succeeding in accumulating instability in the atmosphere.

Chapter 5 Conclusion

By means of examining spatial SM-P feedbacks temporally and spatially in ERA5, the most important finding in this study is before significant precipitation occurs, no matter the reason is, positive (negative) coupling does have had higher moisture (temperature) anomaly already accumulated for several days in the low atmosphere while enough positive temperature (moisture) anomaly also has co-existed. Second, MSE and CAPE pile up mostly on the previous day under positive coupling while under negative coupling, they soar even higher merely on the event day morning. Third, CIN under negative coupling cases is stronger than that under positive ones on the event day morning, which needs extra force, that is, stronger convection, to break the energy barrier above. Last but not least, there are mainly three other phenomena which may help trigger the final rainfall, two on the previous day and the other on the event day: (a) moisture and temperature gathering under both coupling in daytime in temporal and spatial perspectives, (b) pioneering rainfall happened in the previous night which may extra moisten the air, and (c) rapidly moistening in the event day morning from bottom to top under positive coupling while from top to bottom under negative coupling. The correspondence shows that previous days information may be of crucial use to the prediction of precipitation and takes part in land-atmosphere interaction, which was scarcely discussed in the past. Moreover, the additional knowledge of how SM-P coupling develops proposed here may help us better understand the role it plays in the complicated issue “wet gets wetter, dry gets dryer (WWDD)” in climate changes (Zhou et al., 2021). There are still many more relevant variables worth investigating to perfect what we have found here, such as the traits of clouds, wind effect etc. Model experiments like turbulence and causality issues are also required.

Chapter 6 References

[1] Amante, C., and B. W. Eakins (2009). Etopo1 1 arc-minute global relief model: Procedures, data sources and analysis, NOAA Tech. Memo. NESDIS NGDC, 24, 1–19, doi:10.7289/V5C8276M

[2] Bartholomé, E., and A. S. Belward (2005). GLC2000: A new approach to global land cover mapping from Earth observation data, Int. J. Remote Sens., 26(9), 1959–1977, doi:10.1080/01431160412331291297

[3] Climate Data Store, ERA5: Fifth generation of ECMWF atmospheric reanalyses of the global climate (2017)

[4] Eltahir, E. A. B. & Bras, R. L. (1996). Precipitation recycling. Rev. Geophys. 34, 367–378

[5] Findell, K.L., Eltahir, E.A.B. (1997). An analysis of the soil moisture-rainfall feedback, based on direct observations from Illinois. Water Resour. Res. 33 (4), 725–735

[6] Fitzharris, Blair (2001). Global energy and climate processes. In Sturman, A.P. and Spronken-Smith, R. A. (Ed.). The Physical Environment: A New Zealand Perspective (pp. 113-129). Melbourne: Oxford University Press

[7] Froidevaux, P., Schlemmer, L., Schmidli, J., Langhans, W., & Schär, C. (2013). Influence of the background wind on the local soil moisture– precipitation feedback. Journal of the Atmospheric Sciences, 71(2), 782–799

[8] Garcia-Carreras, L., D. J. Parker, C. M. Taylor, C. E. Reeves, and J. G. Murphy (2010). Impact of mesoscale vegetation heterogeneities on the dynamical and thermodynamic properties of the planetary boundary layer. J. Geophys. Res., 115, D03102, doi:10.1029/2009JD012811

[9] Garcia-Carreras, L., Parker, D. J. & Marsham, J. H. (2011). What is the mechanism for the modification of convective cloud distributions by land surfaceinduced flows? J. Atmos. Sci. 68, 619634

[10] Guillod, B. P., et al. (2015). Reconciling spatial and temporal soil moisture effects on afternoon rainfall, Nat. Commun., 6, doi:10.1038/ ncomms7443

[11] Holgate, C. M., Van Dijk, A. I. J. M., Evans, J. P., & Pitman, A. J. (2019). The importance of the one-dimensional assumption in soil moisture - Rainfall depth correlation at varying spatial scales. Journal of Geophysical Research: Atmospheres, 124, 2964–2975. https:// doi.org/10.1029/2018JD029762

[12] Hsu, H., M.-H. Lo, B. P. Guillod, D. G. Miralles, and S. Kumar (2017). Relation between precipitation location and antecedent/subsequent soil moisture spatial patterns, J. Geophys. Res. Atmos., 122, doi:10.1002/2016JD026042

[13] Kiehl, J. T., and K. E. Trenberth (1997): Earth's annual global mean energy budget. Bull. Amer. Meteor. Soc., 78, 197-208

[14] Klein, C., and C. M. Taylor (2020). Dry soils can intensify mesoscale convective systems. Proc. Natl. Acad. Sci. USA, 117, 21 132–21 137, https://doi.org/10.1073/pnas.2007998117

[15] Koster, R.D., et al. (2004). Regions of strong coupling between soil moisture and precipitation. Science 305, 1138–1140

[16] Lee, J. M., Zhang, Y., & Klein, S. A. (2019). The effect of land surface heterogeneity and background wind on shallow cumulus clouds and the transition to deeper convection. Journal of the Atmospheric Sciences, 76(2), 401–419

[17] Miralles, D. G., Holmes, T. R. H., De Jeu, R. A. M., Gash, J. H., Meesters, A. G. C. A., and Dolman, A. J. (2011). Global land-surface evaporation estimated from satellite-based observations, Hydrol. Earth Syst. Sci., 15, 453–469,

https://doi.org/10.5194/hess-15-453-2011

[18] Nicholson, S.E. (2015). Nicholson Evolution and current state of our understanding of the role played in the climate system by land surface processes in semi-arid regions Glob. Planet. Change, 133, pp. 201-222

[19] Seneviratne, S. I., T. Corti, E. L. Davin, M. Hirschi, E. B. Jaeger, I. Lehner, B. Orlowsky, and A. J. Teuling (2010). Investigating soilmoisture-climate interactions in a changing climate: A review, Earth-Sci. Rev., 99(3–4), 125–161, doi:10.1016/j.earscirev.2010.02.004

[20] Taylor, C. M., F. Saïd, and T. Lebel (1997). Interactions between the land surface and mesoscale rainfall variability during HAPEX-Sahel. Mon. Wea. Rev., 125, 2211–2227

[21] Taylor, C.M., Lebel, T. (1998). Observational evidence of persistent convective-scale rainfall patterns. Mon. Weather Rev. 126, 1597–1607

[22] Taylor, C.M., Ellis, R.J. (2006). Satellite detection of soil moisture impacts on convection at the mesoscale. Geophys. Res. Lett. 33, L03404

[23] Taylor, C. M., D. J. Parker, and P. P. Harris (2007). :An observational case study of mesoscale atmospheric circulations induced by soil moisture. Geophys. Res. Lett., 34, L15801, doi:10.1029/2007GL030572

[24] Taylor, C. M., A. Gounou, F. Guichard, P. P. Harris, R. J. Ellis, F. Couvreux, and M. De Kauwe (2011). Frequency of Sahelian storm initiation enhanced over mesoscale soil-moisture patterns, Nat. Geosci., 4, 430–433, doi:10.1038/ngeo1173

[25] Taylor, C. M., R. A. M. de Jeu, F. Guichard, P. P. Harris, and W. A. Dorigo (2012). Afternoon rain more likely over drier soils, Nature, 489, 423–426, doi:10.1038/nature11377

[26] T. Foken (2008). The energy balance closure problem: an overview Ecol. Appl., 18

(6), pp. 1351-1367

[27] Wei, J., Su, H. & Yang, ZL. (2016). Impact of moisture flux convergence and soil moisture on precipitation: a case study for the southern United States with implications for the globe. Clim Dyn 46, 467–481

[28] Welty, J., Stillman, S., Zeng, X., & Santanello, J. (2020). Increased likelihood of appreciable afternoon rainfall over wetter or drier soils dependent upon atmospheric dynamic influence. Geophysical Research Letters, 47, e2020GL087779

[29] Zhou, S., Williams, A.P., Lintner, B.R. et al. (2021). Soil moisture–atmosphere feedbacks mitigate declining water availability in drylands. Nat. Clim. Chang. 11, 38–44. https://doi.org/10.1038/s41558-020-00945-z

Diagrams

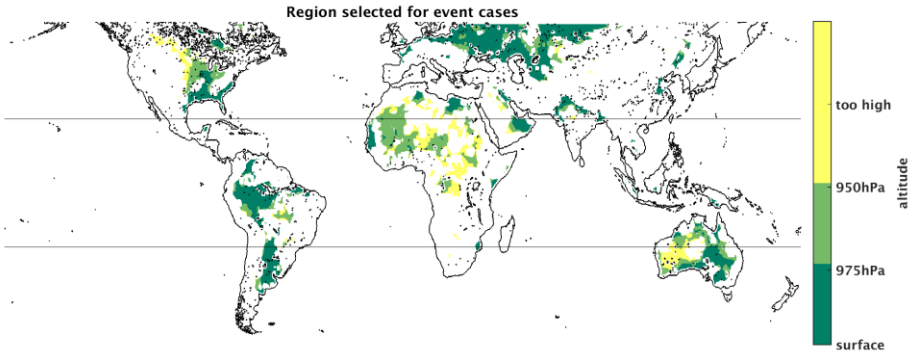

Figure 1. The region filtered for rain events. Rain events are only picked out from the region of dark and light green color. Yellow one is the region above 950hPa (600m altitude), uncolored land regions are too steep (altitude difference >300m within the 5x5 box), and the rest contains water body more than 5% within the 5x5 box (lake may illustrate like black dot if it is too small).

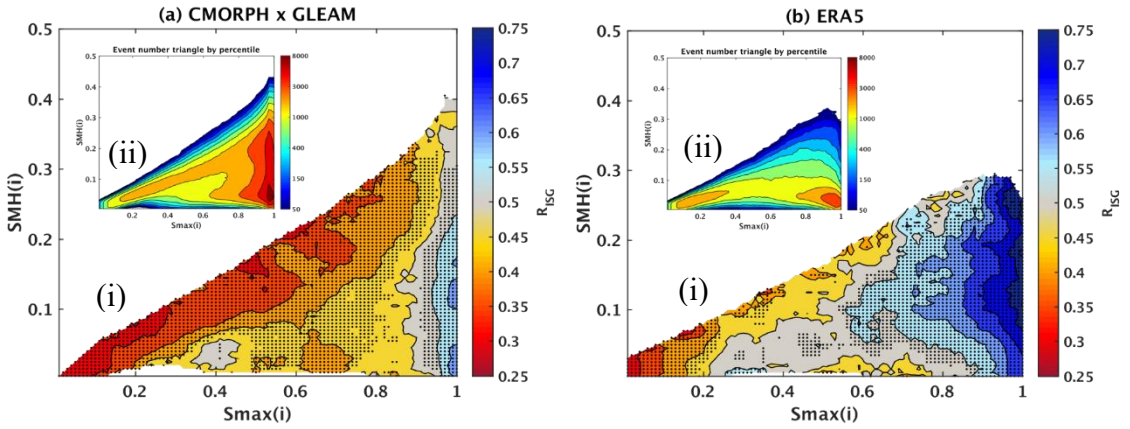

Figure 2. (i. The ratio of cases that is positive ISG (R_{ISG}) coupled with soil moisture condition using (a. observation data and (b. ERA5 reanalysis, modified from Hsu et al., 2017. X-axis and y-axis are the maximum soil moisture (Smax) and the soil moisture heterogeneity (SMH) defined by the standard deviation of SM both within the 5x5 box, respectively. Shading is R_{ISG}. Dots denote the ratio pass the 0.05 significant Z-test on both sides, based on the null assumption that the ratio = 0.5. (ii. Case number corresponding to main diagram using (a. observation data and (b. ERA5 reanalysis.

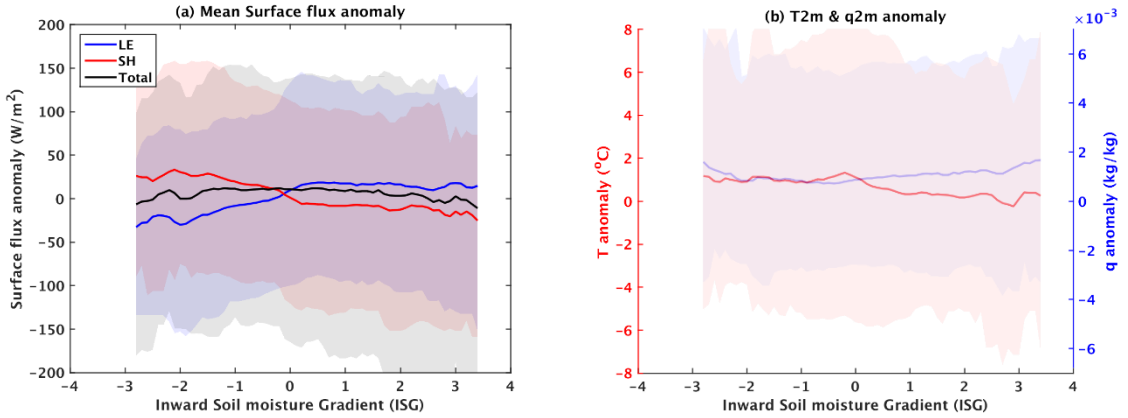

Figure 3. Composite temporal conditions at L_{00} at 11am changed with ISG (x-axis) at (a. surface where red, blue and black lines are upward mean sensible, latent and total heat flux (sensible heat pluses latent heat flux) anomaly, respectively; and (b. near surface, where red line illustrates near surface temperature anomaly (using left y-axis) and blue line specific humidity anomaly (using right y-axis) both at 2m height. Light shading area shows the 95% cases spread of corresponding each color lines. Only 99.99% of the events that is closer to 0 are painted. Seasonality is removed before averaging.

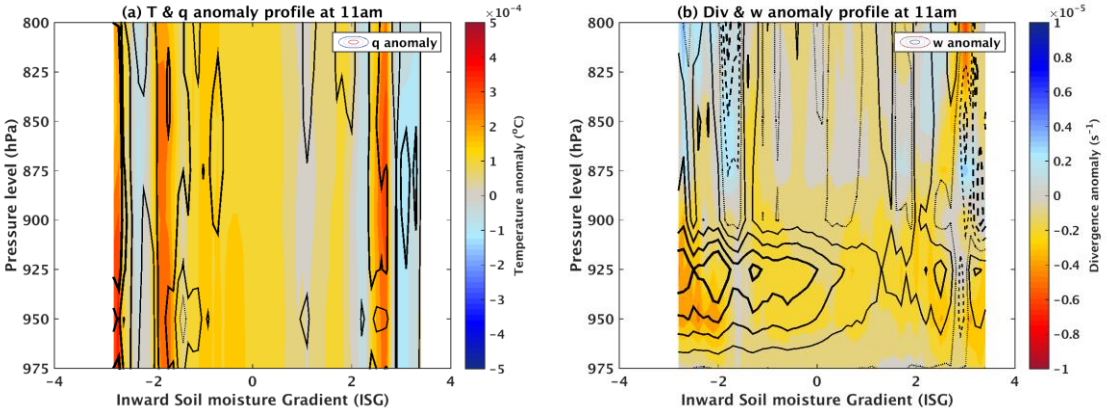

Figure 4. Composite vertical temporal atmospheric conditions of (a. thermal state where shading is temperature anomaly and contour is specific humidity anomaly; and (b. dynamic state where shading is divergence anomaly and contour is vertical velocity anomaly at L_{00} at 11am in the event morning changed with ISG (x-axis) and pressure level(y-axis). Solid, dashed and dotted contour lines denote positive, negative and zero value, respectively, which get coarser as value grows extreme with interval of $3 \times 10^{-11}(kgkg^{-1})$ for q anomaly and $0.0008(ms^{-1})$ for w anomaly. Only 99.99% of the events that is closer to 0 are painted.

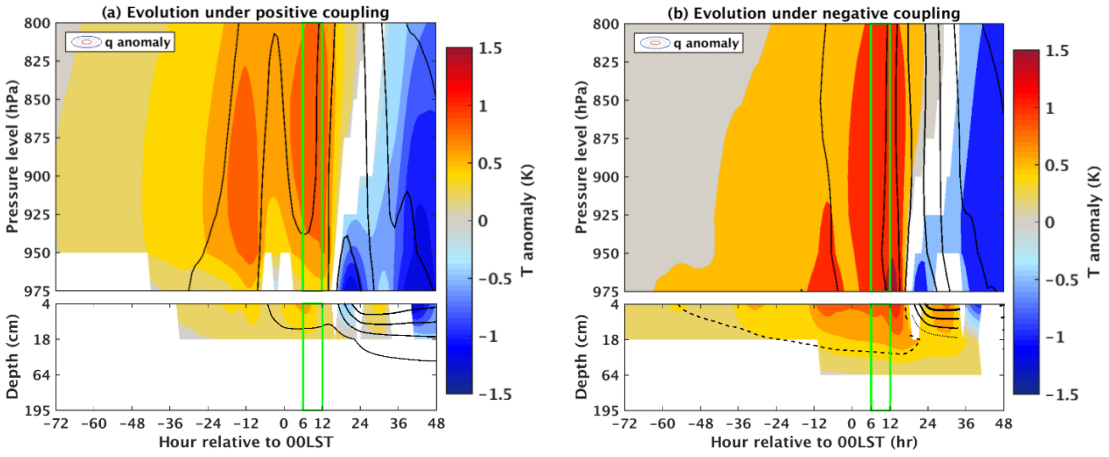

Figure 5. Composite evolution of vertical temporal thermal condition at L_{00} in the atmosphere and land from 3 days before (-72hr) the event day to 1 day after (+48hr) under (a. positive spatial SM-P coupling and (b. negative spatial SM-P coupling. Shading is temperature(K) anomaly. Contour is specific humidity anomaly(kg/kg) in the upper panel while volumetric soil water anomaly(m3/m3) in the lower one. Coarser solid(dashed) line indicated higher positive(negative) value with interval of 0.0004 for q anomaly and 0.01 for SM anomaly. Dotted line symbolizes zero. Only shading and contour that passes 95% confident level using t-test are shown. Green box highlights the event morning (6-11LST). Noted that y-axis in lower panel is depth below ground surface in cm.

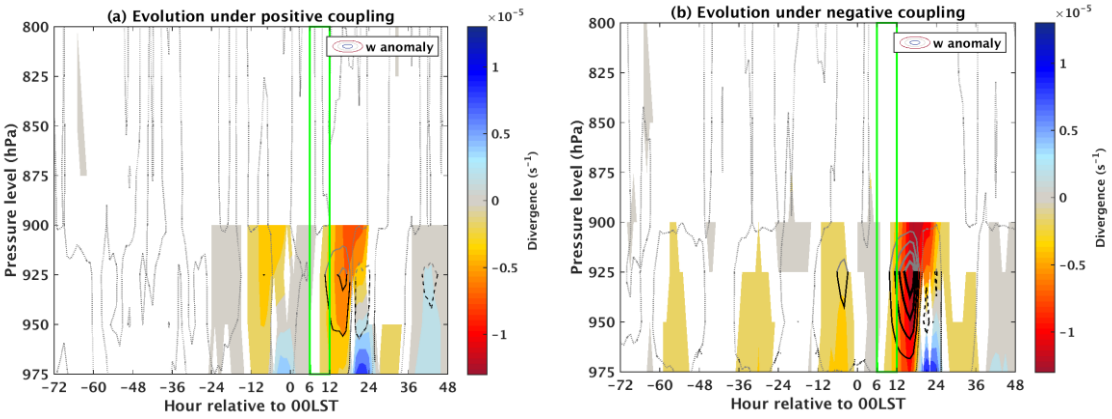

Figure 6. Composite evolution of vertical temporal dynamic condition at L_{00} in the atmosphere from 3 days before (-72hr) the event day to 1 day after (+48hr) under (a. positive spatial SM-P coupling and (b. negative spatial SM-P coupling. Shading is divergence anomaly. Contour is vertical velocity anomaly. Coarser solid(dashed) line indicated higher positive(negative) value with the interval of $0.0012(s^{-1})$. Results that pass 95% confident level using t-test are shaded or contoured in black. Green box highlights the event morning (6-11LST).

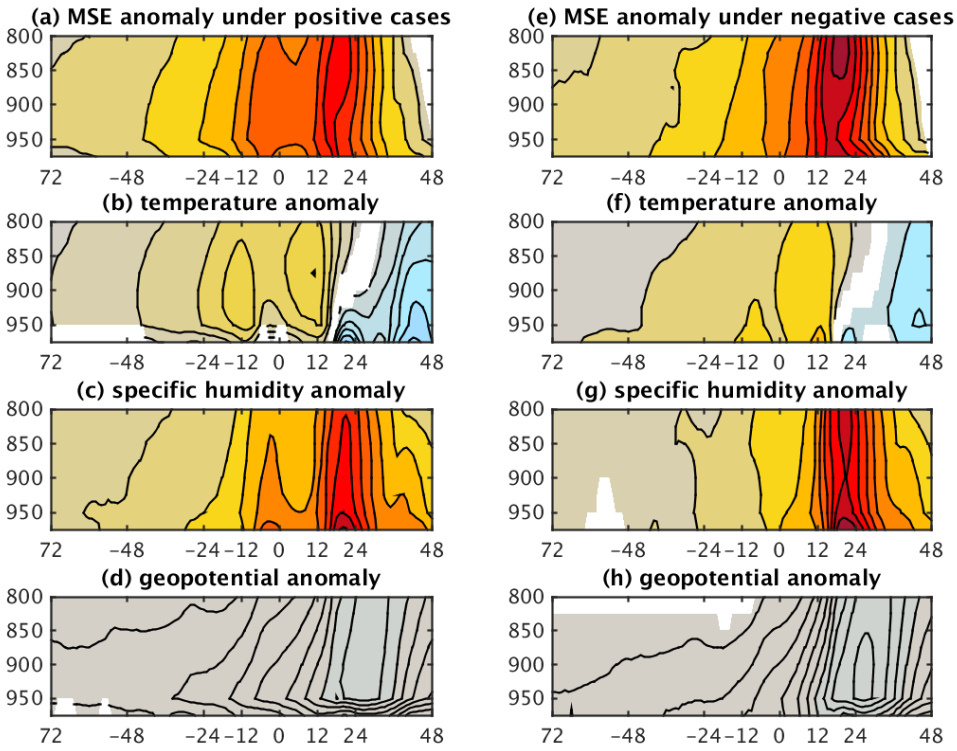

Figure 7, Composite evolution of temporal (a., (e., MSE(Moist Static Energy) and three contributors including (b., (f., temperature anomaly, (c., (g., specific humidity anomaly, and (d., (h., geopotential anomaly at L_{00} in the atmosphere from 3 days before (-72hr) the event day to 1 day after (+48hr) under (a., b., c., d., positive spatial SM-P coupling and (e., f., g., h., negative spatial SM-P coupling. Only shading that passes 95% confident level using t-test are shown.

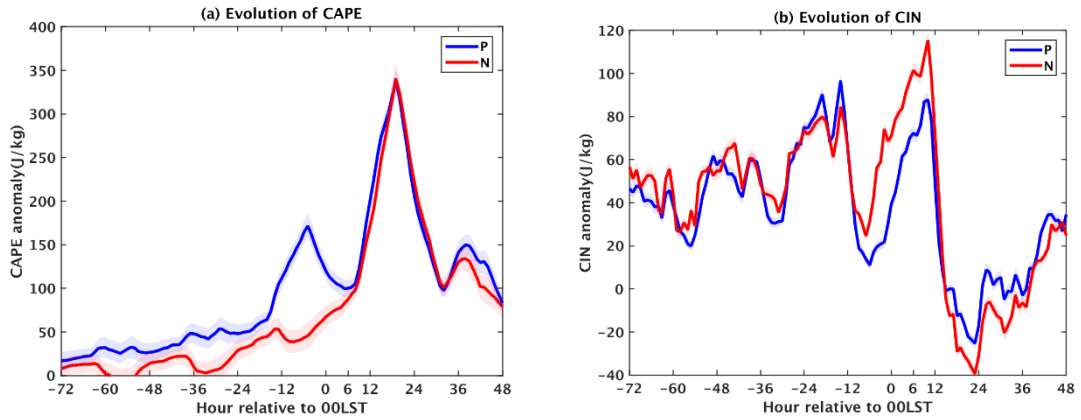

Figure 8. Composite evolution of (a. CAPE and (b. CIN anomaly in temporal perspective. Blue and red lines represent the values under positive and negative coupling from 3 days before (-72hr) the event day to 1 day after (+48hr). Shading is the range that passes 95% significant T-test on both sides, based on the null assumption that the value = 0. Besides, nan values existing in CIN are not counted in.

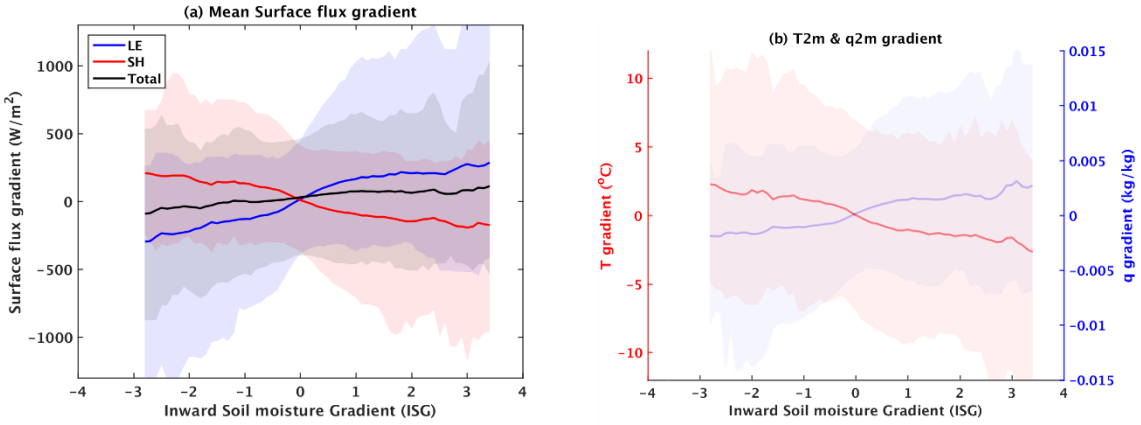

Figure 9. Composite spatial conditions at 11am changed with ISG (x-axis) at (a. surface where red, blue and black lines are upward mean sensible, latent and total heat flux (sensible heat pluses latent heat flux) gradient, respectively; and (b. near surface, where red line illustrates near surface temperature gradient (using left y-axis) and blue line specific humidity gradient (using right y-axis) both at 2m height. Variables are calculated by inward gradient instead of anomaly. Other captions are same as figure 3.

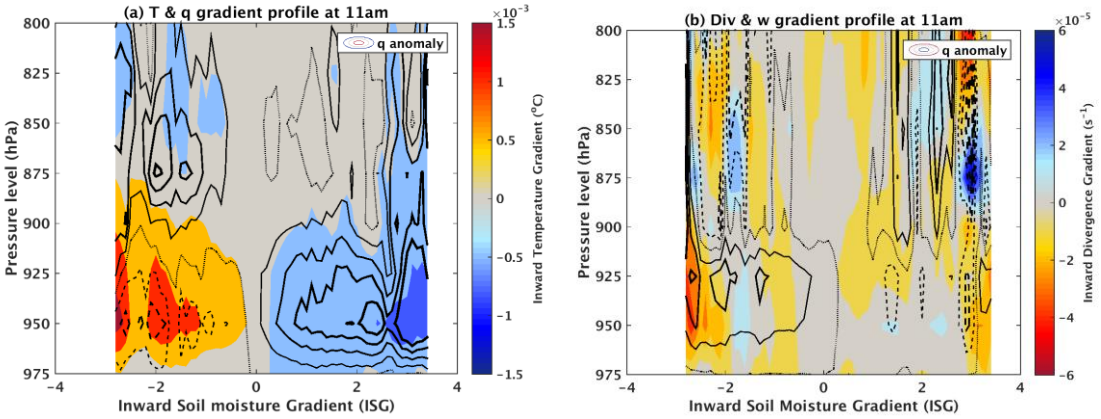

Figure 10. Composite vertical spatial atmospheric conditions of (a. thermal state where shading is temperature gradient and contour is specific humidity gradient; and (b. dynamic state where shading is divergence gradient and contour is vertical velocity gradient at 11am in the event morning changed with ISG(x-axis) and pressure level(y-axis). Variables are calculated by inward gradient instead of anomaly. Contour intervals are $10^{-10}(kgkg^{-1})$ for q gradient and $0.006(ms^{-1})$ for vertical velocity gradient. Other captions are same as figure 4.

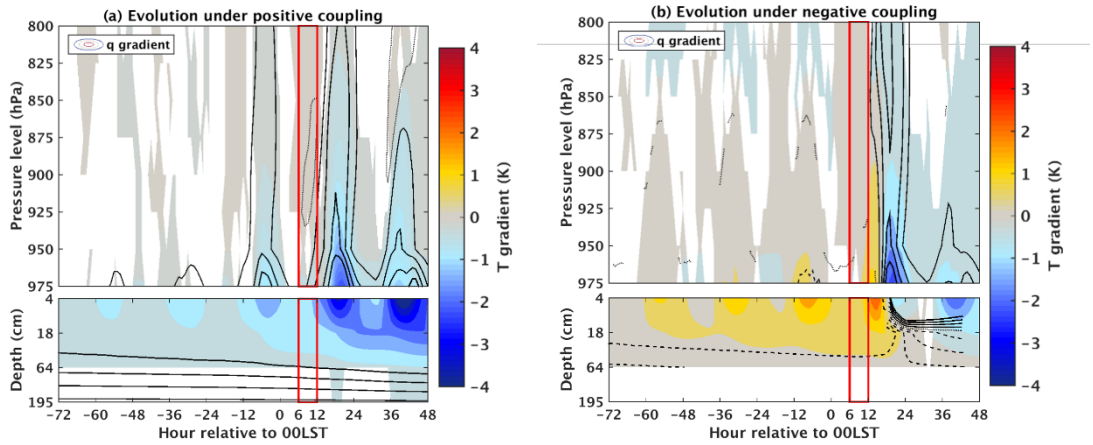

Figure 11. Composite evolution of vertical spatial thermal condition at L_{00} in the atmosphere and land from 3 days before (-72hr) the event day to 1 day after (+48hr) under (a. positive spatial SM-P coupling and (b. negative spatial SM-P coupling. Variables are calculated by inward gradient instead of anomaly. Contour intervals are 0.0004 for q gradient and 0.01 for SM gradient. Except for the box color is replaced by red to better illustrate, other captions are same as figure 5.

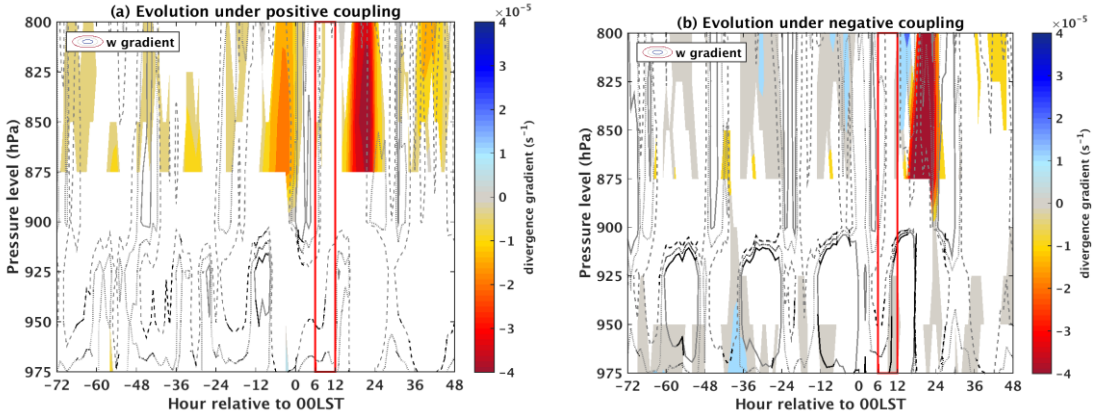

Figure 12. Composite evolution of vertical spatial dynamic condition at L_{00} in the atmosphere from 3 days before (-72hr) the event day to 1 day after (+48hr) under (a. positive spatial SM-P coupling and (b. negative spatial SM-P coupling. Variables are calculated by inward gradient instead of anomaly. Contour interval is 0.001. Except for the box color replaced by red to better illustrate, other captions are same as figure 6.

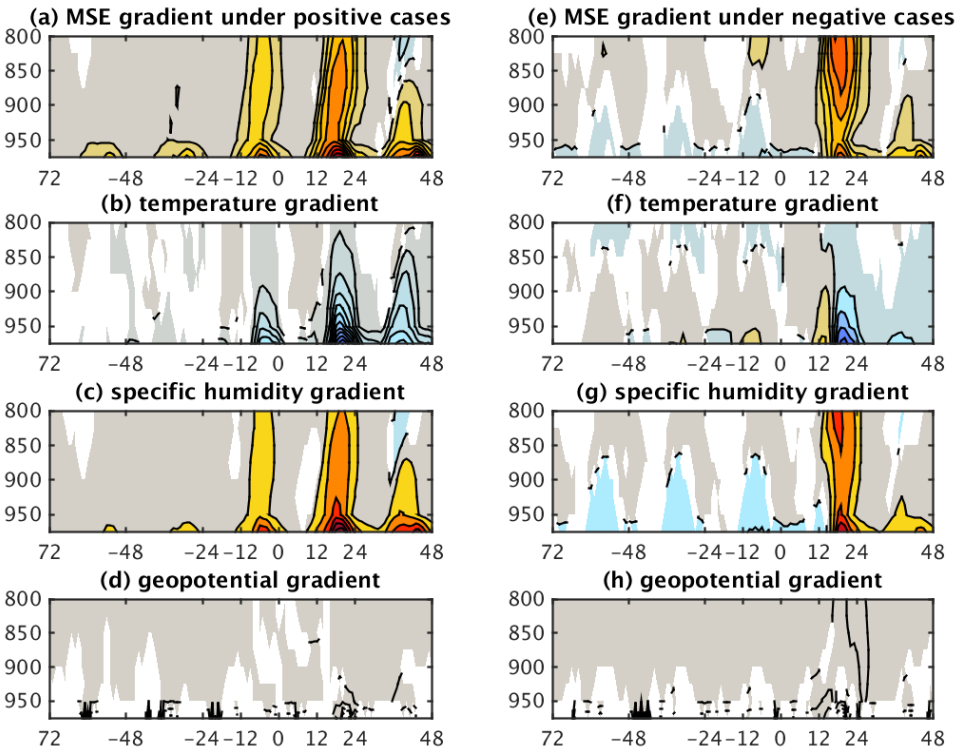

Figure 13. Composite evolution of spatial (a., (e., MSE(Moist Static Energy) and three contributors including (b., (f., temperature gradient, (c., (g., specific humidity gradient, and (d., (h., geopotential gradient at L_{00} in the atmosphere from 3 days before (-72hr) the event day to 1 day after (+48hr) under (a., b., c., d., positive spatial SM-P coupling and (e., f., g., h., negative spatial SM-P coupling.

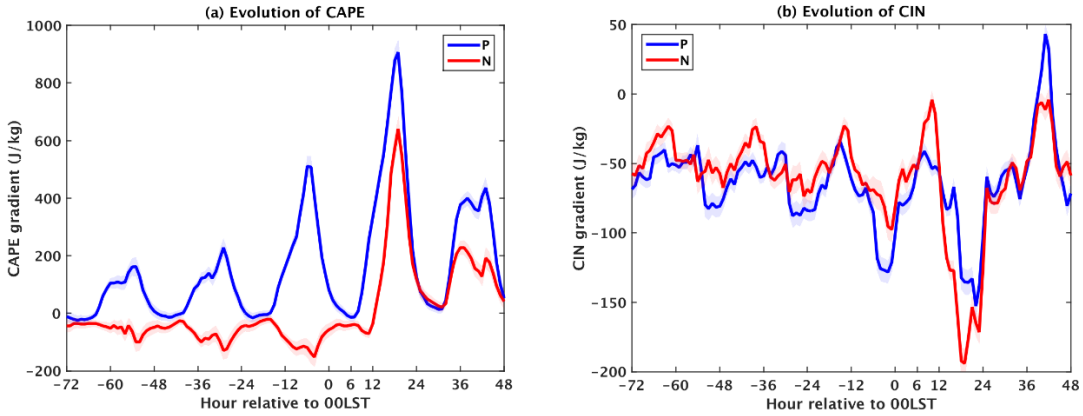

Figure 14. Composite evolution of (a. CAPE and (b. CIN gradient in spatial perspective.

Captions are same as figure 8.

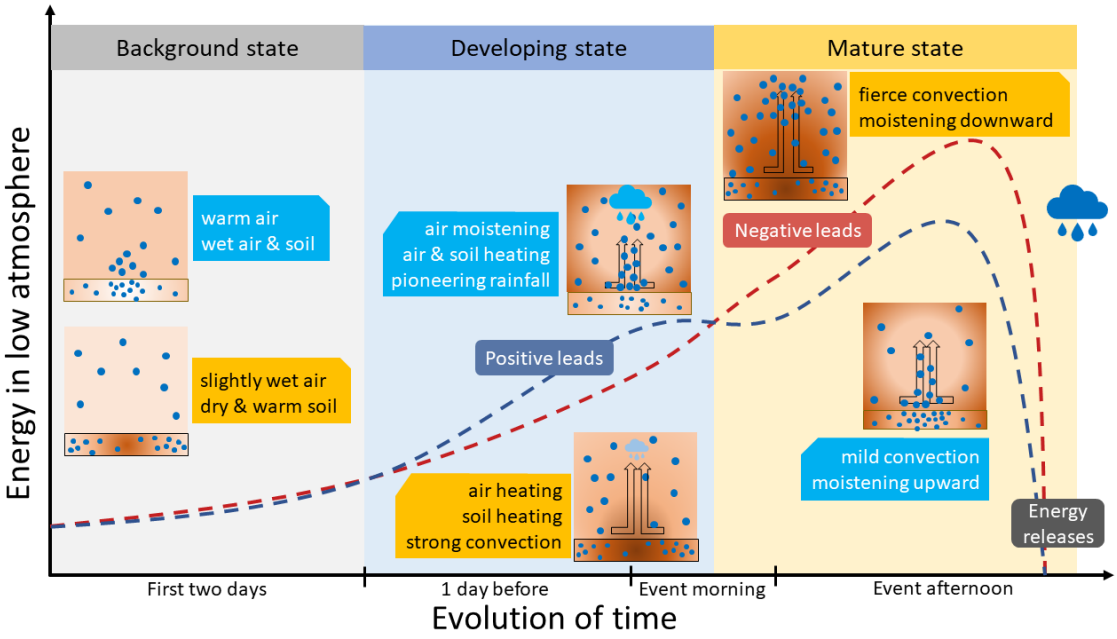

Figure 15. Schematic diagram of the evolution of preconditions under positive and negative spatial SM-P coupling. Dashed lines represent the change of MSE in low atmosphere where blue one is positive coupling and red one is negative. Three rectangular background color boxes describe three states before the event: Background state, developing state and mature state. Descriptions with cool color is for positive coupling while with warm color is for negative. As for the inserted figures, darker color means warmer temperature anomaly while more intense blue dots indicate higher moisture anomaly.